

Response of cross- and tee-shaped concrete column sections to combined flexure and axial loading

Winston Onsongo

Most reinforced concrete columns are square or rectangular in shape. For such, comprehensive design charts and software are available to enable design for combined compression and uniaxial bending. The columns designed to support loads such as those in multistorey apartment buildings are usually much wider than the thickness of masonry walls that are invariably part of the building construction system. However, it may be architecturally desirable to neatly blend the columns with the walls. This requires the columns to have the same thickness as the walls and these columns may then have to be tee- or cross-shaped. As an aid to the design of such columns, this presents a comparative study of the predicted response to combined compression and uniaxial bending for the cross- and tee-shaped sections having the same cross section area and reinforcement content as an equivalent square section. It is shown that the cross- and tee-sections can effectively replace the square section.

INTRODUCTION

Square or rectangular columns and beams cast monolithically with reinforced concrete slabs constitute a common popular form of structural support for modern high-rise buildings. For such standard column cross sections, the designer has readily available comprehensive and familiar design aids in the form of charts and design software. The square cross section is indeed an efficient shape for a column carrying a predominant axial loading.

The columns are often designed to act together with load-bearing walls, particularly for office or residential high-rise buildings. For such buildings external walls and main internal partition walls demarcate the desired functional spaces and the columns are preferably located at the intersection points of the walls. In such cases it may be desirable on aesthetic considerations to match the width of the columns with the adjacent wall thickness so as to avoid columns sticking out of wall planes. This will require cross- or tee-shaped columns that blend neatly with the walls, as shown in figure 1. In contrast the equivalent square columns would jut out, as they would be wider than the thickness of the walls.

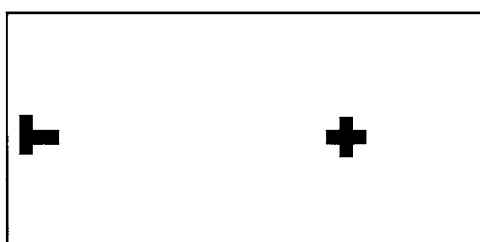


Figure 1

If a designer chooses to use cross or tee-shaped columns instead of square or rectangular cross sections, the designer will not have readily available design charts to use and the general response to combined bending and axial loading of such shapes will be unfamiliar. The objective of this paper is to present the predicted response to combined bending and axial loading using well-known theoretical models for cross- and tee-column sections and to compare the response to that for a comparable square section.

Details of column sections studied

The details of the sections used in the study are shown in figure 2:

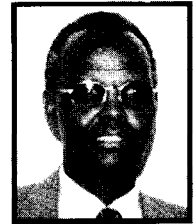
	BS	BX1	BX2	BT/BT1
A (mm ²)	160 000	160 000	160 000	160 000
A _s (mm ²)	2 412(12Y16)	2 412(12Y16)	2 412(12Y16)	2 412(12Y16)
r _{cy} (mm)	115,46	119,46	119,46	119,46
r _{sy} (mm)	117,27	120,54	122,86	120,54

Figure 2 Column cross section details

With respect to figure 2 the reader should note that:

- All the cross sections have the same cross section area and the same reinforcement content. The concrete cover to the centroid of the reinforcing bar is 40 mm.
- The dimensions of BX1, BX2 (which will be referred to as X-type sections) and BT (which will be referred to as T-type section) have

WINSTON MARASI ONSONGO is a registered professional engineer in South Africa and Professor and Director of



Undergraduate Engineering Education at the University of the Witwatersrand. He graduated in civil engineering from Canterbury University in New Zealand in 1969 and obtained his master's degree (1972) and doctorate (1978) in structural engineering from the University of Toronto, Canada. He has over twenty years of university teaching experience in structural engineering and has worked on many projects as a consulting structural engineer.

been chosen to match a wall thickness of 200 mm.

- Section BT is the T-type section shown with the bending moment applied to cause compression in the top flange face, whereas BTI is the same section but with bending moment applied to cause compression in the bottom stem face.

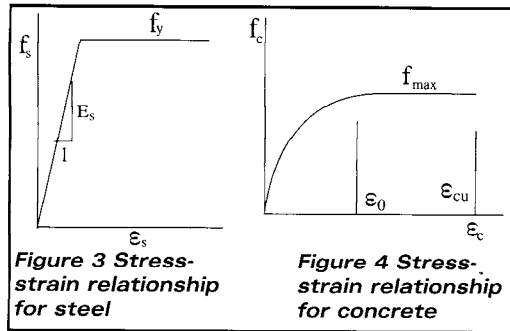
- r_{cy} is the minimum radius of gyration of the plain section ignoring the reinforcing steel, whereas r_{sy} is the radius of gyration of the section taking the reinforcing steel into account. In determining r_{sy} , the modulus of elasticity of concrete has been taken as $E_c = 26 \text{ kN/mm}^2$ and the modulus of elasticity for the reinforcing bars has been taken as $E_s = 200 \text{ kN/mm}^2$. The concrete cylinder strength (about 80 – 90% of cube strength) is assumed to be $f'_c = 30 \text{ MPa}$, and the yield stress for reinforcing steel is assumed to be $f_y = 460 \text{ MPa}$.

- As column slenderness is inversely proportional to the minimum radius of gyration, the X-type and T-type sections are stiffer than the square section BS with respect to buckling.

Stress-strain characteristics of steel and concrete

The well-known theoretical model based on 'plane sections remain plane' assumption is capable of predicting the complete response of structural concrete sections subjected to combined flexure and axial loading. For accurate predictions, the theoretical model requires accurate stress-strain characteristics of the materials. The theory will be used to predict the failure interaction curves for the BS, BX1, BX2, BT, and BTI sections shown in figure 2.

It will be assumed that the stress-strain relationship for the reinforcing steel is bilinear as shown in figure 3, and the modulus of elasticity will be taken as 200 kN/mm^2 . The stress-strain relationship for concrete will be assumed to be parabolic over the strain range $0 \leq \epsilon_c \leq \epsilon_o$ and to have constant maximum stress f_{max} over the strain range $\epsilon_o \leq \epsilon_c \leq \epsilon_{cu}$ as shown in figure 4. The strain ϵ_o is taken to be equal to the strain corresponding to the maximum compressive stress in a standard concrete cylinder test. This strain ϵ_o has been established from tests to be approximately 0,002 over a wide range of concrete strengths. Moreover, compressive strains of 0,003 to 0,0045 normally occur before a beam fails under flexure and hence we shall take the concrete compressive strain at failure ϵ_{cu} to be 0,0035 for theoretical predictions. We shall take the maximum compressive stress f_{max} to be $0,85 f'_c$ and the maximum steel stress f_y in tension or compression to be 460 MPa for the comparative study.



Solution procedure

For any given section the following procedure has been used to predict sets of axial force and bending moment that acting together would fail the section and thus define a point on the failure interaction curve:

- Choose a strain profile with a maximum compressive strain of ϵ_{cu} in the most compressed face, as shown in figure 5(b). The most compressed face will be referred to as the compression face. Such a strain profile presumes that plane sections before loading remain plane after loading and that there is perfect bond between the steel and concrete.
- From the chosen strain profile and using the defined stress-strain relationships for steel and concrete (see figures 3 and 4), the corresponding stresses are determined to be as shown in figure 5(c). Note that the tensile stresses in concrete are ignored.

- The steel stresses acting on the steel bar section areas result in forces and the force in bar 'i' can be evaluated as:

$$F_{si} = f_{si} A_{si} \quad (1)$$

where $f_{si} = \epsilon_{si} E_s$ for $\epsilon_{si} < \epsilon_y$
and $f_{si} = f_y$ for $\epsilon_{si} \geq \epsilon_y$

The force F_{si} will act at the location of the bar at depth y_{si} from the compression face. The resultant tension force in all the bars is determined as

$$F_{st} = \sum F_{si} \quad (2)$$

The resultant tension force F_{st} will act at a depth y_s from the compression face and

$$y_s = \sum F_{si} y_{si} / F_{st} \quad (3)$$

- The summation of the elementary forces $f_c dA$ due to the compressive stresses f_c acting on the concrete section will give a resultant compressive force F_{cc} . The concrete stresses are

defined as:

$$f_c = f_{max} (2\Omega - \Omega^2) \text{ for } 0 \leq \Omega \leq 1,0$$

$$f_c = f_{max} \text{ for } \Omega > 1,0$$

where $\Omega = \epsilon_c / \epsilon_o$ (4)

For a rectangular section of width b and assuming a strain profile with the neutral axis depth c from the compression face (see figure 6) F_{cc} can be deduced as

$$F_{cc} = f_{max} bc \left((c_1 / c) + 2 / (3\Omega_u) \right)$$

where $\Omega_u = \epsilon_{cu} / \epsilon_o$ and $c_1 =$ depth over which maximum stress f_{max} acts. (5)

The position at which F_{cc} acts from the compression face is y_c determined as

$$y_c = f_{max} bc^2 \left(0,5 (c_1 / c)^2 + 2 / (3\Omega_u) - 5 / (12 \Omega_u^2) \right) / F_{cc} \quad (6)$$

- From the resultant tension force in the steel and the resultant compression force in the concrete the net axial compression force on the column section is determined as:

$$P = F_{cc} - F_{st} \quad (7)$$

- If the plastic centroid of the section is located at y_p from the compression face, the moment about the centroid acting together with the axial force P can be determined as

$$M = F_{st} (y_s - y_p) + F_{cc} (y_p - y_c) \quad (8)$$

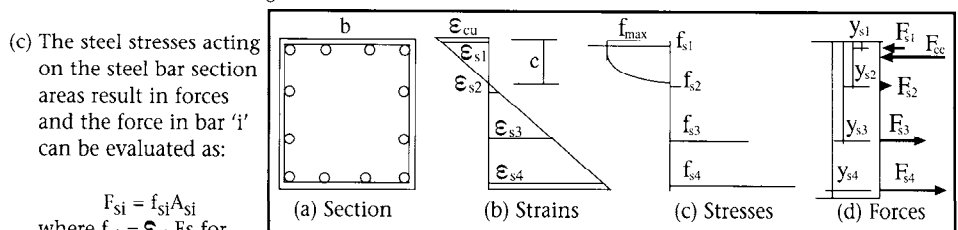


Figure 5 Solution procedure

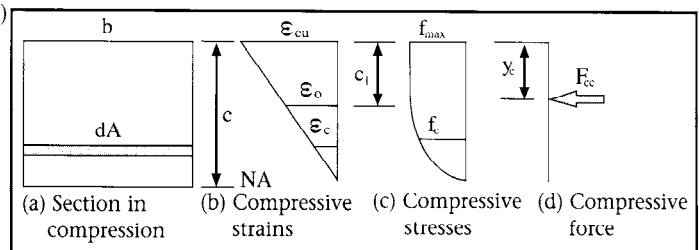


Figure 6 Evaluation of F_{cc}

Determination of failure interaction curves

The solution procedure outlined above has been used to predict the failure interaction curves shown in figures 7 and 8. The procedure was programmed to generate sets of moment and axial loads that would give rise to a maximum compressive strain of ϵ_{cu} in the compression face. The differences in the geometry of the

cross sections studied were taken into account in the evaluation of the resultant compression forces F_{cc} by the computer program. Five reference points on the interaction curve for a given section were first determined and this was followed by the determination of as many intermediate points as necessary to define the curve. The reference points were

- 1 The pure flexure case with zero axial force (M_{u0})
- 2 The balanced failure case (M_{ub}, P_{ub})
- 3 The case with zero strain at the 'bottom' face opposite to the face with maximum compression (M_{u1}, P_{u1})
- 4 The case with compressive strain equal to ϵ_o in the bottom face (M_{u2}, P_{u2})
- 5 The pure axial compression case (P_{u0})

It should be noted that with the assumed stress-strain relationship for concrete, case 4 will give the same axial force as for case 5 if all the steel bars are in the post yield range. Moreover, the predicted capacities do not include design factors normally specified in codes of practice to determine reliable design strengths.

Predicted response

Figure 7 shows the predicted failure interaction curves for the square section and the X-type sections. Figure 8 shows similar plots for BS, BT, and BTI. The values of moment and axial force sets for the five reference points on each of the interaction curves are summarised in table 1.

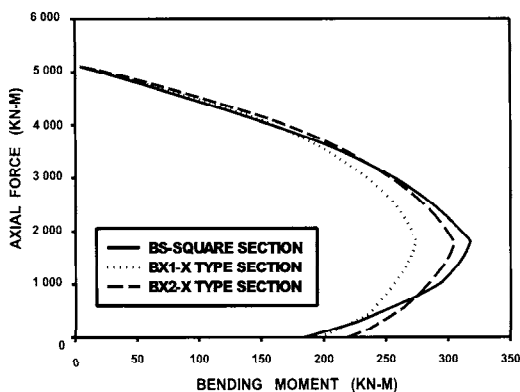


Figure 7 Bending moment / axial force interaction for BS, BX1, and BX2

Examination of figure 7 and table 1 reveals that the interaction curve for BX2 is very similar to that of BS. Note that both BX1 and BX2 have pure moment capacities larger than that of BS, but the axial loading enhances the moment carrying capacity of the square section

much more than for the X-type section. Thus at axial load levels close to balanced failure, the square section has a moment capacity greater than that of either BX1 or BX2.

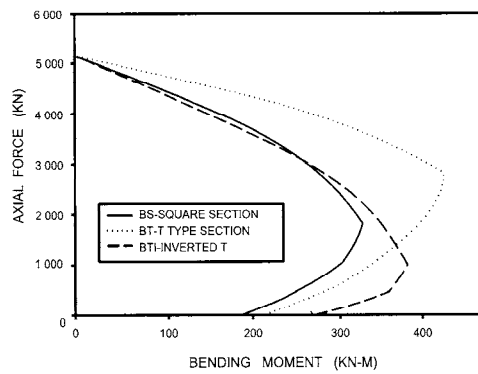


Figure 8 Bending moment / axial force interaction for BS, BT, and BTI

Figure 8 shows that the T-section will resist substantially larger moments than the square section over the entire interaction curve. The inverted T-section – whose response is also shown – resists larger moments than the square section for axial load levels below the balanced failure loading, but for higher axial loads the response of BTI is close to that of BS.

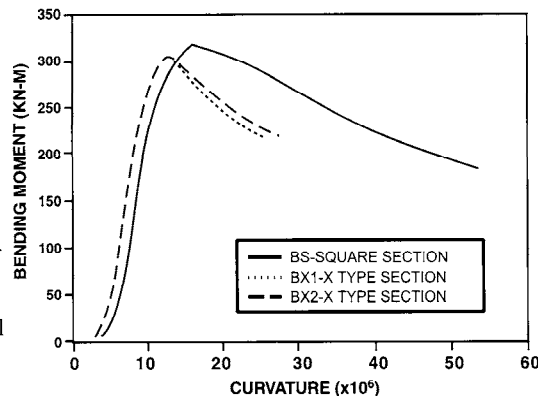


Figure 9 Moment / curvature plot for BS, BX1, and BX2

Figure 9 shows the failure moment-curvature plots for the square and for the X-type sections. The peak on the curves corresponds to the balanced failure point and the maximum curvature corresponds to the pure flexure case. These plots indicate that the response at failure of BX1 and BX2 are very similar and for axial load levels smaller than that at balanced failure, the square section displays much greater curvature than the X-type section for the same moment. Thus BX1 and BX2 have greater flexural stiffness than BS. This characteristic is even more clearly revealed by figure 10, where using the moment at balanced failure and the corresponding curvature as the base moment ratios are plotted against curvature ratios. The plot shows that the curvature of BS for pure flexure is over three times the curvature at balanced failure, whereas for the X-type sections the curvature for pure flexure is about twice that at balanced failure.

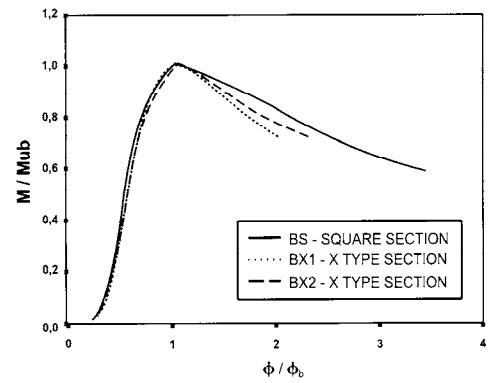


Figure 10 Moment ratio / curvature plot for BS, BX1, and BX2

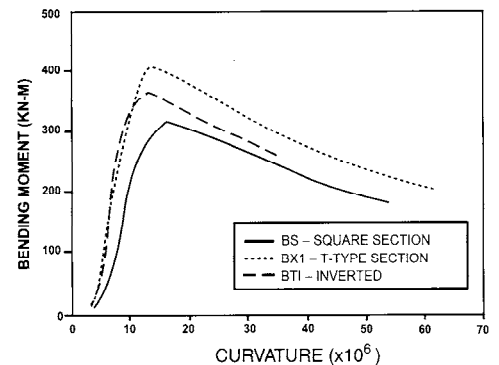


Figure 11 Moment ratio / curvature plot for BS, BT, and BTI

Figure 11 shows the failure moment-curvature plots for the square and for the T-type sections. Note that for the same curvature the T-type sections resist higher moments than the square section. Figure 12, which is similar to Figure 10 discussed above, shows that for axial load levels below the balanced failure, the T-type sections display greater curvature for the same moment than the square section.

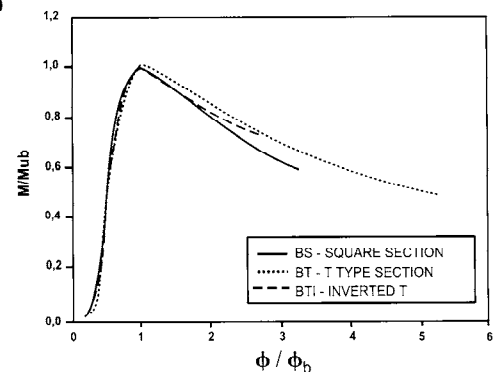


Figure 12 Moment ratio / curvature plot for BS, BT, and BTI

CONCLUSION

The moment-axial load interaction curves and the plots involving curvature reveal some differences between the response of the square section and the X-type and T-type sections. However, the differences indicate some advantage in using the X-type and T-type sections. The symmetric X-type section can replace an interior

square column with the advantage of greater stiffness, and with judicious steel layout the X-type section can resist greater moments at the same axial load level than the square section. The T-type section will provide suitable external columns that will match with external walling. Such external columns are often subjected to greater bending moments than the internal columns. The interaction curves show that the T-type section will provide greater moment resistance than the square section at the same axial load level and this is advantageous. Thus it is concluded that the X-type and T-type column sections can effectively replace square or rectangular sections to achieve more desirable finishes.

Interaction curves suitable for the design of X-type and T-type column sections can be obtained by introducing the relevant safety factors specified in codes of prac-

tice. Alternatively, theoretical interaction curves such as those predicted in this paper can be used if appropriate safety

factors are incorporated into the design loads.

Table 1 Moment and axial force values at reference points

Ref. point	1	2		3		4		5
Section	Muo (kN-m)	Mub (kN-m)	Pub (kN)	Mu1 (kN-m)	Pu1 (kN)	Mu2 (kN-m)	Pu2 (kN)	Puo (kN)
BS	184,4	317,8	1 810	162,4	3 964	3,8	5 104	5 128
BX1	196,8	274,1	1 806	132,4	4 235	3,0	5 114	5 128
BX2	219,4	305,0	1 778	144,6	4 201	4,5	5 106	5 128
BT	209,3	407,1	2 821	192,2	4 337	7,5	5 099	5 128
BTI	265,4	367,4	999	212,2	3 438	4,6	5 099	5 128

References

ACI Committee 1989. Building code requirements for reinforced concrete (ACI 318-89), Detroit: American Concrete Institute.

Cranston, W B 1972. *Analysis and design of reinforced concrete columns*. Cement and Concrete Association, Research Report 20.

Park, R and Paulay, T 1975. *Reinforced Concrete Structures*. Wiley.

